International Journal of Innovative
Computing, Information and Control
Volume **15**, Number **6**, December **2019**

 ISSN 1349-4198
pp. **2119–2133**

SLIDING MODE PREDICTION FAULT-TOLERANT CONTROL METHOD BASED ON WHALE OPTIMIZATION ALGORITHM

Zhangxi Liu, Pu Yang, Dejie Li and Mengyang Xu

College of Automation
Nanjing University of Aeronautics and Astronautics
No. 29, Jiangjun Avenue, Jiangning District, Nanjing 210016, P. R. China
ppyang@nuaa.edu.cn

Received April 2019; revised August 2019

Abstract. *A novel fault-tolerant control method for sliding mode prediction based on whale optimization algorithm is designed for fault-tolerant control of quad-rotor aircraft system with discrete time-delay uncertainties. The whole process sliding surface is used as the prediction model to ensure the global robustness, and a power function reference trajectory with fault compensation is designed to suppress the influence of chattering and suppress the uncertainty and fault. In the process of rolling optimization, considering the high-precision and fast response of the optimization process, the whale optimization algorithm is adopted, which has strong optimization performance, less parameter setting, fast convergence and high precision. The simulation shows that the algorithm has good effects in terms of robustness, weakening of chattering, and convergence speed.*
Keywords: Fault tolerant control, Time varying delay, Whale optimization algorithm, Power function approach rate, Quad-rotor helicopter

1. **Introduction.** With the development of science and technology, today's society has largely become a society driven by various smart devices. In the long-term operation of smart devices, a series of faults often occurs under the influence of external factors. In order to enable the agent to operate safely under fault conditions, fault-tolerant control technology for dealing with fault problems is booming and has some results in dealing with practical problems. Fault-tolerant control has been developed into two directions: active fault tolerance and passive fault tolerance [1-4]. Many strategies have been proposed in dealing with actuators and sensor faults [5,6].

In fact, the four-rotor drone has entered daily life and has demonstrated its indispensable value in agriculture, military, transportation, and tracing. In recent years, the field of automatic control has proposed quite a number of practical control strategies for the formation flight of UAVs [7], tracking and obstacle avoidance, such as sliding mode control, predictive control, adaptive control, and sliding mode predictive control. Of course, various challenges have emerged during the research process. First of all, when studying the four-rotor discrete system, the control difficulty and the complexity of the control algorithm are greatly aggravated due to the interference during flight and the error of system modeling. Secondly, the faults that exist during the flight, the time lag [8] in the system make the control more difficult.

Research on discrete control systems has become an important component of the control field. It has great exploration value for fault diagnosis and fault-tolerant control of discrete systems. The algorithm proposed in [9] robustly controls the single-input single-output system and solves the control problem of uncertain systems that do not satisfy

DOI: 10.24507/ijicic.15.06.2119

the matching condition. Paper [10] has been improved for paper [11], although it can be applied to a multiple input multiple output system, but does not consider external interference, and has certain limitations. Paper [11] proposes an adaptive tracking control method based on reinforcement learning for a class of unknown multi-input multi-output nonlinear discrete systems with few learning parameters. The remarkable feature of this method is that it reduces the cost of fault-tolerant process, reduces the number of learning parameters, and thus reduces the amount of calculation. However, this method only considers a simple MIMO model, which is difficult to be applied in practice. In paper [12], for the uncertain discrete nonlinear system, an explicit high-order sliding mode predictive control algorithm is adopted. The method has good stability and converges faster than the traditional sliding mode prediction algorithm. However, this paper does not consider the time lag that is common in practical systems. Regrettably, the existence of time lag often exacerbates the complexity of the system, but many control algorithms do not take it into account when designing the design.

Since the time lag affects the control performance in real systems, many researchers now consider the effects of time lag in the process of algorithm design. A sliding mode prediction algorithm [13] is adopted for systems with time delay and parameter perturbation. This method has strong anti-interference ability and stability, and it is also effective in dealing with time lag. This paper only considers the effect of time-invariant delay on the system, but does not analyze and research time-varying delay. For the time-delay constraint system [14], the model predictive control method is designed to deal with the time-delay problem. The neural dynamic optimization is adopted to improve the optimization precision and optimization speed, and strengthen the online optimization ability of model predictive control, but the same problem is that only fixed time lags are considered. Aiming at the state time lag and input time lag in aero-engine [15], a sliding mode prediction algorithm based on time-delay compensator is designed. This method provides a new idea for how to deal with the time lag problem. However, the external interference encountered by the aero-engine has not been dealt with. The model of the system only considers the influence of time lag. The more common system parameter perturbation is not processed, and it is difficult for the actual system to have no disturbance. In paper [16], the linear sliding surface is designed as the sliding mode prediction model, and it is difficult to avoid the instability phenomenon that may occur in the approaching process. In the process of rolling optimization, only the extreme value necessary condition is used to find the control law. This method is computationally intensive and the accuracy is not satisfactory. Paper [17] comprehensively considers time lag, faults and disturbances. A discrete sliding mode prediction fault-tolerant control method based on multi-agent particle swarm optimization is designed. The sliding mode chattering is effectively suppressed, and the particle swarm optimization algorithm is also adopted in the optimization problem.

In paper [17], the linear sliding mode surface is designed as a prediction model because the global stability cannot be guaranteed by the sliding mode approach process. The reference trajectory is not particularly ideal in dealing with chattering. In the optimization process, the particle swarm optimization algorithm is adopted. The algorithm has complex operation flow and is easy to fall into local minimum values, and the effect is not good in convergence speed and convergence precision. Aiming at the above problems, this paper makes improvement, designs a new control algorithm and compares with it. Compared with [17], this paper designs a fault-tolerant algorithm to deal with uncertain systems with time-varying state delays, and designs the global sliding mode switching function [18] as a sliding mode prediction model to avoid the instability of the approach process. The global robustness is guaranteed, the reference trajectory of power function with fault and

uncertainty compensation is designed, the buffeting is weakened to a greater extent, and the whale optimization algorithm [19] is designed to optimize on the rolling optimization problem. Compared with Particle Swarm Optimization (PSO), this algorithm has faster convergence speed and more accurate solution accuracy.

The rest of this article is organized as follows. In Section 2, the model of the design object is proposed, and some reasonable assumptions are made which are consistent with the actual object. In Section 3, an effective new control algorithm is designed, the controller is designed, and the control law is solved. Then, in Section 4, the stability analysis is given and the rationality of the algorithm is proved. Finally, in Section 5, we use four-rotor aircraft model to verify the effectiveness of the algorithm and add the comparison of simulation curves to highlight the advantages of the algorithm designed in this paper. In Section 6, the work of this paper is summarized and some prospects for future work are presented.

2. **Problem Statement and Preliminaries.** In this paper, the mathematical model of Qball-X4 four-rotor helicopter developed by Quanser Company of Canada is adopted [20]. Considering the model of the X/Y direction channel of the quadrotor system, due to the geometric symmetry of the quadrotor, the motion in the Y direction can be called a symmetrical X-direction motion, so generally only the motion in the X direction is considered for analysis and modeling. When the quadrotor is moving in the X direction, it is affected by the total lift and pitch angle, and assuming the yaw angle is 0, the model can be obtained (1):

$$\begin{cases} F = K_g \dfrac{\omega}{s+\omega} u \\ \nu = \dfrac{\omega}{s+\omega} u \\ \dot{v} = -\omega\nu + \omega u \\ M_g \ddot{X} = 4F\sin(\theta) \\ \begin{bmatrix} \dot{X} \\ \ddot{X} \\ \dot{\nu} \end{bmatrix} = \begin{bmatrix} 0 & 1 & 0 \\ 0 & 0 & \dfrac{4K_g}{M_g}\theta \\ 0 & 0 & -\omega \end{bmatrix} \begin{bmatrix} X \\ \dot{X} \\ \nu \end{bmatrix} + \begin{bmatrix} 0 \\ 0 \\ \omega \end{bmatrix} u \end{cases} \tag{1}$$

where, F is lift, K_g is positive gain, ω is the actuator bandwidth, u is the actuator input, M_g is the quad-rotor mass, θ is pitch angle, ν is the new state variable introduced. Let $\sin(\theta) = \theta$, and the above model can be obtained. The above is an ideal model for the direction of the four-rotor. After discretizing this model, consider system perturbation, external disturbances, faults, time lags, etc. We can build the following model (2):

$$\begin{cases} x(k+1) = (A+\Delta A)x(k) + (B+\Delta B)u(k) + (A_d+\Delta A_d)x(k-\tau(k)) \\ \qquad\qquad + w(k) + Ef(k) \\ y(k) = Cx(k) \end{cases} \tag{2}$$

ΔA, ΔB, ΔA_d are the internal perturbation of the system, $x(k) \in R^n$, $u(k) \in R^p$, $y(k) \in R^q$, are the state, input and output of the system. $w(k) \in R^n$ is external disturbance of the system, $f(k)$ is fault function, $\tau(k)$ is the time varying delay of the systemupper and lower bound of it is $[0, \tau_u]$, A, B, C, E, A_d are the constant matrices.

Let

$$d(k) = \Delta A x(k) + \Delta B u(k) + \Delta A_d x(k-\tau(k)) + w(k) + Ef(k) \tag{3}$$

$d(k)$ is the uncertainty and failure of the system, and unknown. So one-step delay estimation method is used to obtain $\hat{d}(k)$ approximately as follows:

$$d(k) = d(k-1) = x(k) - Ax(k-1) - A_d x(k-1-\tau(k-1)) - Bu(k-1) \tag{4}$$

System (2) can be rewritten as follows:

$$\begin{cases} x(k) = Ax(k) + Bu(k) + A_d x(k-\tau(k)) + d(k) \\ y(k) = Cx(k) \end{cases} \tag{5}$$

This paper considers the additive fault of the actuator. For the quadrotor, its actuator is its drive system, namely, four small motors. Therefore, according to the actual situation, the fault of the four small motors must be within a reasonable range, and the rate of change of the fault is also bounded. Now make the following reasonable assumptions for $d(k)$:

Assumption 1: The fault and uncertainty of the system have an upper and lower bound. $d_L \leq |d(k)| \leq d_U$;

Assumption 2: The rate of change of the fault and uncertainty of the system is bounded. $|d(k) - d(k-1)| \leq d_0$.

3. Algorithm Design.

3.1. Sliding mode prediction model design.

Different from paper [17], a new global sliding mode switching function is designed in this paper to eliminate the approaching process, which will have better robustness and stability. The global sliding mode switching function is designed, so that the initial state of the system state trajectory is located on the switching surface, eliminating the linear sliding mode approaching process and ensuring the global robustness of the system.

$$s(k) = \sigma y(k) - \alpha^k \sigma y_0 = \sigma C x(k) - \alpha^k \sigma C x_0 \tag{6}$$

where $y(k)$ is actual output, σ is designed by pole assignment [21], x_0 is the initial state of the system, y_0 is the output when the system is in the initial state. It can be known from (6) that $s(0) = 0$, the system state trajectory at the initial moment is located at the switching plane. $\alpha \in (0, 1)$, and it is a constant. The sliding mode prediction model based on the state of the system is (7).

$$s(k+1) = \sigma C x(k+1) - \alpha^{k+1} \sigma C x_0 \tag{7}$$

The nominal system of system (5) is as follows:

$$x(k) = Ax(k) + Bu(k) + A_d x(k-\tau(k)) \tag{8}$$

The predicted output of the prediction model at the moment $(k+P)$ can be obtained according to systems (7), and (8).

$$\begin{aligned} s(k+p) &= \sigma C x(k+p) - \alpha^{k+p} \sigma C x_0 \\ &= \sigma C \left[A^P x(k) + \sum_{i=1}^{P} A^{i-1} A_d x(k+p-i-\tau(k+p-i)) \right. \\ &\quad \left. + \sum_{i=1}^{M-1} A^{P-i} B u(k+i-1) + \sum_{i=1}^{P-M} A^i B u(k+M-1) \right] - \alpha^{k+p} \sigma C x_0 \end{aligned} \tag{9}$$

where P is the prediction time domain, and M is the control time domain, and $M \leq P$, $u(k+j) = u(k+M-1)$ $(j = M-1, \ldots, P)$. The vector form of (9) is:

$$S_{PM}(k) = \Omega X(k) + \Xi U(k) + \Psi X_d(k) - \Gamma X_0 \tag{10}$$

where

$$
\begin{aligned}
&S_{PM}(k) = [s(k+1), \ldots, s(k+p)]^T \\
&X(k) = [x(k+1), \ldots, x(k+p)]^T \\
&X_0 = [x_0, \ldots, x_0]^T \\
&U(k) = [u(k), u(k+1), \ldots, u(k+M-1)]^T \\
&\Omega = \left[(\sigma CA)^T, \ldots, \left(\sigma CA^P\right)^T\right]^T \\
&\Xi = \begin{bmatrix}
\sigma CB & 0 & \cdots & \cdots & 0 \\
\sigma CAB & \sigma CB & 0 & \cdots & 0 \\
\vdots & \vdots & \cdots & \cdots & \vdots \\
\sigma CA^{M-1}B & \sigma CA^{M-2}B & \cdots & \sigma CAB & \sigma CB \\
\sigma CA^M B & \sigma CA^{M-1}B & \cdots & \sigma CA^2 B & \sigma CAB + \sigma CB \\
\vdots & \vdots & \cdots & \vdots & \vdots \\
\sigma CA^{P-1}B & \sigma CA^{P-2}B & \cdots & \sigma CA^{P-M+1}B & \sum_{i=0}^{P-M} \sigma CA^i B
\end{bmatrix} \\
&\Gamma = \left[\alpha^k, \alpha^{k+1}, \ldots, \alpha^{k+P}\right]^T \\
&\Psi = \begin{bmatrix}
\sigma CA_d & 0 & \cdots & \cdots & 0 \\
\sigma CAA_d & \sigma CA_d & & & 0 \\
\vdots & \vdots & \ddots & & \vdots \\
\vdots & \vdots & & \ddots & \vdots \\
\sigma CA^{P-1}A_d & \sigma CA^{P-2}A_d & \cdots & \cdots & \sigma CA_d
\end{bmatrix}
\end{aligned}
$$

3.2. **Feedback correction design.** Due to some uncertain factors such as external interference in the actual quad-rotor system, model predictive control is usually only used to implement the control quantity at the current moment. At the next moment, according to the actual output or state information of the controlled object, the feedback strategy should be adopted to modify or compensate the prediction model, and then the new optimization should be performed. It is not difficult to see that without the feedback strategy of predictive control, the predictive control system can be regarded as an open loop control system, which leads to a large prediction error and seriously affects the control accuracy. Therefore, the design of feedback strategy is particularly important to form an overall closed-loop optimal control loop. Therefore, according to Equation (9), we can deduce the prediction output of $(k-P)$ moment k to moment, that is, to predict the output of k moment by p-step prediction from $(k-P)$ moment. The output value of the sliding mode prediction model for k moment from $(k-P)$ moment can be deduced:

$$
\begin{aligned}
s(k|k-P) = \sigma C \Bigg[& A^P x(k-P) + \sum_{i=1}^{P} A^{i-1} A_d x(k-i-\tau(k-i)) \\
& + \sum_{i=1}^{M-1} A^{P-1} B u(k-P+i-1) + \sum_{i=1}^{P-M} A^i B u(k-P+M-1) \Bigg] \\
& - \alpha^k \sigma C x_0
\end{aligned}
\tag{11}
$$

Then, the error between the actual output and the predicted output at moment k is as follows, and add the error as a correction to the prediction model:

$$
\begin{aligned}
e(k) &= s(k) - s(k|k-P) \\
\tilde{s}(k+P) &= s(k+P) + j_p e(k)
\end{aligned}
\tag{12}
$$

The vector form of (12) is as follows:

$$\tilde{S}_{PM}(k) = S_{PM}(k) + J_p E(k) \tag{13}$$

where,

$$J_p = \begin{bmatrix} j_1 & & & \\ & j_2 & & \\ & & \ddots & \\ & & & j_p \end{bmatrix}$$

j_p is the correction coefficient, as the prediction step increases, j_p decreases in turn, $j_1 = 1, j_1 > j_2 > \cdots > j_p > 0$.

3.3. **Reference trajectory design.** In the sliding mode predictive control, the selection of the reference trajectory can be constructed according to the sliding mode approach rate, so how to reduce the influence of chattering becomes a problem that needs careful consideration when selecting. Because of the good effect of the power function in weakening the chattering, this paper uses the power function as the reference trajectory. At the same time, considering the influence of faults and uncertainties, the design of the reference trajectory is embedded with the suppression method to maximize the compensation for faults and uncertainties.

$$\begin{aligned} s_{ref}(k+1) &= (1-\varsigma)s_{ref}(k) - \varepsilon f(s_{ref}(k), \beta, \delta) - \xi(k) + \xi_1 \\ s_{ref}(k) &= s(k) \end{aligned} \tag{14}$$

where, $f(s_{ref}(k), \beta, \delta) = \begin{cases} |s_{ref}(k)|^{\beta}\mathrm{sgn}(s_{ref}(k)), & |s_{ref}(k)| \geq \delta \\ \dfrac{s_{ref}(k)}{\delta^{1-\beta}}, & |s_{ref}(k)| < \delta \end{cases}$, sgn() is sign function.

The range of values of each parameter is as follows, $0 < \beta < 1$, $0 < \delta < 1$, $\delta > \left(\frac{\varepsilon}{1-\varsigma}\right)^{\frac{1}{1-\beta}}$, $0 < \left(\frac{\varepsilon}{1-\varsigma}\right) < 1$. $\xi(k)$ is the influence of system uncertainty and fault on the output value of sliding mode, is compensation for system uncertainty and fault:

$$\begin{aligned} \xi(k) &= \sigma C d(k) = \sigma C[\Delta A x(k) + \Delta B u(k) + \Delta A_d x(k - \tau(k)) + w(k) + E f(k)] \\ \xi_1 &= \frac{\xi_U + \xi_L}{2} = \frac{\sigma C d_U + \sigma C d_L}{2} \end{aligned} \tag{15}$$

The vector form of system (14) is:

$$S_{ref}(k) = [S_{ref}(k+1), S_{ref}(k+2), \ldots, S_{ref}(k+P)]^T \tag{16}$$

3.4. **Rolling optimization design.** The selection of optimization performance index is the most important part of rolling optimization, which involves the future behavior of the system and future control strategy. The control strategy designed in this paper requires the future output to closely follow the expected reference trajectory, so the designed performance index minimizes the variance between the output value and the expected value. The optimization cost function is defined as:

$$j(k) = \sum_{i=1}^{P} \lambda_i \left[s_{ref}(k+i) - \tilde{s}(k+1)\right]^2 + \sum_{l=1}^{M} \gamma_l [u(k+l-1)]^2 \tag{17}$$

where, λ_i and γ_l are weight coefficients.

The vector form of Equation (17) can be written as:

$$J(k) = \left[S_{ref}(k) - \tilde{S}_{PM}(k)\right]^T Q \left[S_{ref}(k) - \tilde{S}_{PM}(k)\right] + \left[U^T R U\right] \tag{18}$$

where, $Q = \begin{bmatrix} \lambda_1 & & & \\ & \lambda_2 & & \\ & & \ddots & \\ & & & \lambda_P \end{bmatrix}$, $R = \begin{bmatrix} \gamma_1 & & & \\ & \gamma_2 & & \\ & & \ddots & \\ & & & \gamma_M \end{bmatrix}$. Q and R are weighted diagonal matrices.

3.5. **Optimization algorithm design.** In recent years, various novel intelligent optimization algorithms have been proposed, and bio-optimization algorithms have been widely used and applied in many fields. The Whale Optimization Algorithm (WOA) is a new type of optimization algorithm proposed by Mirjalili of Griffith University in Australia, which is proposed in 2016. The algorithm has many advantages such as simple principle, less parameter setting and strong optimization performance. Comparing whale optimization algorithm and particle swarm optimization algorithm [17], WOA algorithm is superior to particle swarm optimization algorithm in solving accuracy and convergence speed. Therefore, the whale optimization algorithm is designed for rolling optimization.

The purpose of rolling optimization is to obtain $U(k)$ that makes $J(k)$ take a minimum value. Therefore, Equation (18) is taken as the objective function, that is, the optimization performance index $J(k)$ is taken as the fitness function.

The whale optimization algorithm is divided into three stages, whale-enveloped predation, whale bubble predation (local search phase), and whale random search for prey (global search phase).

1) Encircling prey

The whale identifies the prey location and surrounds it. The WOA assumes that the current optimal candidate solution is the target prey, and updates the location of the candidate solution according to the following mathematical model:

$$\begin{cases} \vec{D} = \left| \vec{C}\vec{X}^* - \vec{X}(t) \right| \\ \vec{X}(t+1) = \vec{X}^*(t) - \vec{A}\vec{D} \end{cases} \tag{19}$$

where, $\vec{D}$ is the distance between the individual and the target prey, t indicates the current iteration, $\vec{X}^*(t)$ is the position vector of the best solution obtained so far, $\vec{X}(t)$ is the position vector, $\vec{C}$ and $\vec{A}$ are the coefficient vectors.

The vectors $\vec{C}$ and $\vec{A}$ are calculated as follows:

$$\begin{cases} \vec{C} = 2\vec{r} \\ \vec{A} = 2\vec{a}\vec{r} - \vec{a} \end{cases} \tag{20}$$

In Equation (20), $\vec{r}$ is a random vector in $[0, 1]$, $\vec{a}$ is linearly decreased from 2 to 0 over the course of iterations.

2) Bubble-net hunting method

The whale moves around the prey along the spiral path, spitting out bubble traps and preying. Shrinking encircling mechanism: This behavior is achieved by decreasing the value of $\vec{a}$ from 2 to 0 in Equation (20) over the course of iterations. It can be obtained from Equation (20) that when $\vec{A}$ is located between $[1, 1]$, the next position of the whale can randomly appear at the current position or optimal position, that is, the position at $t + 1$ can be the position at time t, or the global optimal position at time t.

$$\begin{cases} \vec{D}' = \left| \vec{X}^*(t) - \vec{X}(t) \right| \\ \vec{X}(t+1) = \vec{D}' e^{bl} \cos(2\pi l) + \vec{X}^*(t) \end{cases} \tag{21}$$

Equation (21) simulates the spiral hunting of humpback whales, where, b is constant for defining the shape of the logarithmic spiral, l is a random number in $[-1, 1]$. On the

account of the humpback whale swims in a shrinking circle during the predation and along the spiral-shaped path simultaneously. Therefore, in order to simulate this behavior, we assume that the probability 50 percent can choose to reduce the surrounding method or spiral model to update the position of the whale. The mathematical model is described as follows:

$$\vec{X}(t+1) = \begin{cases} \vec{X}^*(t) - \vec{A}\vec{D} & \text{if } \rho < 0.5 \\ \vec{D}' e^{bl} \cos(2\pi l) + \vec{X}^*(t) & \text{if } \rho \geq 0.5 \end{cases} \tag{22}$$

where, ρ is a random number in $[0, 1]$.

3) Random search for prey

When $\left|\vec{A}\right| > 1$, it means that the whale swims outside the shrinking circle. At this time, the whale individual performs a random search. The mathematical model is as follows:

$$\begin{cases} \vec{D} = \left|\vec{C}X_{rand}(t) - X(t)\right| \\ \vec{X}(t+1) = \vec{X}_{rand} - \vec{A}\vec{D} \end{cases} \tag{23}$$

where $\vec{X}_{rand}(t)$ is a random position vector (a random whale) chosen from the current population.

The main parameters of WOA are coefficient vectors $\vec{A}$ and $\vec{C}$, among them, parameter $\vec{A}$ plays an important role in global search and local search. The convergence factor $\vec{a}$ determines the value of $\vec{A}$, larger convergence factors can obtain better global search ability and avoid falling into local optimum, smaller convergence factors are beneficial to local optimization and accelerate the convergence of the algorithm.

4. **Stability Analysis.** From the above rolling optimization process, the control law $U(k)$ that makes $J(k)$ a minimum value can be obtained. The necessary condition for the extreme value of $J(k)$ is $\frac{\partial J(k)}{\partial U(k)} = 0$, so the control law calculated through the WOA must meet it. Therefore, $U(k)$ must meet (24).

$$U(k) = \left[R + \Xi^T Q \Xi\right]^{-1} \Xi^T Q \left[S_{ref}(k) - \Omega X(k) - \Psi X_d(k) + \Gamma X_0 - J_P E(k)\right] \tag{24}$$

Generally, when considering stability, it can be assumed that $R = 0$, and Q is an identity matrix:

$$U(k) = \Xi^{-1} \left[S_{ref}(k) - \Omega X(k) - \Psi X_d(k) + \Gamma X_0 - J_P E(k)\right] \tag{25}$$

For an actual system with faults and uncertainties, the sliding mode predicted output value at time $k + P$ is as follows:

$$S_{PM}(k) = \Omega X(k) + \Xi U(k) + \Psi X_d(k) + \Theta D(k) - \Gamma X_0 \tag{26}$$

where,

$$\Theta = \begin{bmatrix} \sigma C & 0 & \cdots & 0 \\ \sigma CA & \sigma C & \cdots & 0 \\ \vdots & \vdots & \ddots & \vdots \\ \sigma CA^{P-1} & \sigma CA^{P-2} & \cdots & \sigma C \end{bmatrix}, \; D(k) = [d(k), d(k+1), \ldots, d(k+P-1)]^T$$

Then, substituting (25) into (26), gives:

$$S_{PM}(k) = S_{ref}(k) - J_P E(k) + \Theta D(k) \tag{27}$$

In the process of scroll optimization, only the current control input signal acts on the controlled object. So take the first element of the vector expression (27):

$$s(k+1) = s_{ref}(k+1) - j_1(s(k) - s(k|k-1)) + \sigma C d(k) \tag{28}$$

where,

$$\begin{aligned} & s(k)-s(k|k-1) \\ &= \sigma C[x(k)-Ax(k-1)-A_d x(k-1-\tau(k-1))-Bu(k-1)] \\ &= \sigma C d(k-1) \end{aligned} \tag{29}$$

Let $j_1 = 1$, so Equation (28) becomes (30):

$$s(k+1) = s_{ref}(k+1) + \sigma C[d(k)-d(k-1)] \tag{30}$$

From **Assumption 2**, it gives:

$$\begin{cases} |d(k)-d(k-1)| \le d_0 \\ s(k+1) = s_{ref}(k+1) + \sigma C[d(k)-d(k-1)] \le s_{ref}(k+1) + \sigma C d_0 \end{cases} \tag{31}$$

Thereby, substituting (14) into (31), gives:

$$s(k+1) \le s_{ref}(k+1) + \sigma C d_0 = (1-\varsigma)s_{ref}(k) - \varepsilon f(s_{ref}(k),\beta,\delta) - \xi(k) + \xi_1 + \sigma C d_0 \tag{32}$$

Since $\xi(k) = \sigma C d(k)$ and **Assumption 1**: $d_L < |d(k)| < d_U$, we can get $\sigma C d_L < \xi(k) < \sigma C d_U$. Then:

$$s(k+1) \le (1-\varsigma)s_{ref}(k) - \varepsilon f(s_{ref}(k),\beta,\delta) - \sigma C d_L + \xi_1 + \sigma C d_0 \tag{33}$$

And $\xi_1 = \frac{\sigma C d_U + \sigma C d_L}{2}$, then:

$$s(k+1) \le (1-\varsigma)s_{ref}(k) - \varepsilon f(s_{ref}(k),\beta,\delta) - \sigma C d_L + \frac{\sigma C d_U + \sigma C d_L}{2} + \sigma C d_0 \tag{34}$$

Let $\xi_2 = \frac{\sigma C d_U - \sigma C d_L}{2}$,

$$\Lambda = \frac{\sigma C d_U - \sigma C d_L}{2} + \sigma C d_0 = \xi_2 + \sigma C d_0$$

then:

$$s(k+1) \le (1-\varsigma)s_{ref}(k) - \varepsilon f(s_{ref}(k),\beta,\delta) + \Lambda \tag{35}$$

Let:

$$s_{po}(k+1) = (1-\varsigma)s_{po}(k) - \varepsilon f(s_{po}(k),\beta,\delta) \tag{36}$$

So:

$$s(k+1) \le s_{po}(k+1) + \Lambda \tag{37}$$

In summary, we perform stability analysis on $s_{po}(k+1)$.

Proof:

1) When $s_{po}(k) \ge \delta$, then (36) turns to (38).

$$s_{po}(k+1) = (1-\varsigma)s_{po}(k) - \varepsilon {s_{po}}^{\beta}(k) = \left[(1-\varsigma) - \varepsilon {s_{po}}^{(\beta-1)}(k)\right] s_{po}(k) \tag{38}$$

Let $\Delta s_{po}(k) = s_{po}(k+1) - s_{po}(k) = -\varsigma s_{po}(k) - \varepsilon {s_{po}}^{\beta}(k)$, there exists $\frac{\partial \Delta s_{po}(k)}{\partial s_{po}(k)} = -\varsigma - \varepsilon\beta {s_{po}}^{(\beta-1)} < 0$. That is, $\Delta s_{po}(k)$ is the decreasing function of $s_{po}(k)$. When $s_{po} \ge \delta$, we can deduce $\Delta s_{po}(k) = -\varsigma s_{po}(k) - \varepsilon {s_{po}}^{\beta}(k) \le 0$. Obviously, for (38), $s_{po}(k)$ is a decreasing function that converges to $0 \le s_{po}(k) < \delta$. Then, $s_{po}(k+1) \le \vartheta$.

2) When $0 \le s_{po}(k) < \delta$, (36) turns to (39).

$$s_{po}(k+1) = (1-\varsigma)s_{po}(k) - \frac{\varepsilon s_{po}(k)}{\delta^{1-\beta}} \tag{39}$$

Similarly, it is easy to prove $\Delta s_{po}(k) = s_{po}(k+1) - s_{po}(k) \le 0$, so that, $s_{po}(k)$ is a decreasing function, monotonously tends to 0 and does not cross. Then, $s_{po}(k+1) \le \vartheta$.

3) When $-\delta < s_{po}(k) < 0$, (36) turns to (40).

$$s_{po}(k+1) = (1-\varsigma)s_{po}(k) - \frac{\varepsilon s_{po}(k)}{\delta^{1-\beta}} \tag{40}$$

In case of (40), $\Delta s_{po}(k) = s_{po}(k+1) - s_{po}(k) > 0$, so $s_{po}(k)$ is an incremental function that continues to increase until $s_{po}(k) \geq 0$. It can be seen from 2) that once it reaches the range of $s_{po}(k) \geq 0$, $s_{po}(k)$ will converge to 0. Then, $s_{po}t(k+1) \leq \vartheta$.

4) When $s_{po}(k) \leq -\delta$, (36) turns to (41).

$$s_{po}(k+1) = (1-\varsigma)s_{po}(k) - \varepsilon(-s_{po}(k))^{\beta} \tag{41}$$

Let $\Delta s_{po}(k) = s_{po}(k+1) - s_{po}(k) = -\varsigma s_{po}(k) - \varepsilon(-s_{po}(k))^{\beta}$, then $\frac{\partial \Delta s_{po}(k)}{\partial s_{po}(k)} < 0$, $\Delta s_{po}(k) = s_{po}(k+1) - s_{po}(k) > 0$. That is, $\Delta s_{po}(k)$ is the decreasing function of $s_{po}(k)$. When $s_{po}(k) \leq -\delta$, $\Delta s_{po}(k) > 0$. So $s_{po}(k)$ is an incremental function that converges to $0 \leq s_{po}(k) < \delta$. Then, $s_{po}(k+1) \leq \vartheta$.

In summary, we can conclude that there is $k_n < \infty$, for any $k > k_n$, $s_{po}(k+1) \leq \vartheta$ is true. So we can obtain $|s(k+1)| \leq \Lambda + \vartheta$. Therefore, the controller designed in this paper is robust stable.

5. **Experimental Results and Discussions.**

5.1. **Simulation model.**

This paper selects Q-ball produced by Quanser company as the simulation object. Its mathematical model has been given by system (1). In the case of small pitch angle, X axis direction model by linearization without external disturbance, parameter perturbation and time varying delay is obtained as follows:

$$\begin{bmatrix} \dot{X} \\ \ddot{X} \\ \dot{\nu} \end{bmatrix} = \begin{bmatrix} 0 & 1 & 0 \\ 0 & 0 & \frac{4K_g}{M_g}\theta \\ 0 & 0 & -\omega \end{bmatrix} \begin{bmatrix} X \\ \dot{X} \\ \nu \end{bmatrix} + \begin{bmatrix} 0 \\ 0 \\ \omega \end{bmatrix} u \tag{42}$$

When the time delay, parameter perturbation and external disturbance in system (42) are considered, the system model is marked as system (2). Now, each matrix of system (2) is represented as follows:

$$A = \begin{bmatrix} 0 & 1 & 0 \\ 0 & 0 & 12 \\ 0 & 0 & -10 \end{bmatrix}, A_d = \begin{bmatrix} 0 & 0 & 0 \\ 0 & 0 & 4 \\ 0 & 0 & -5 \end{bmatrix}, B = \begin{bmatrix} 0 \\ 0 \\ 15 \end{bmatrix}, E = \begin{bmatrix} 0.1 \\ 0.1 \\ 0.2 \end{bmatrix}, C = \begin{bmatrix} 1 & 0 & 0 \end{bmatrix}$$

The parameter perturbation matrix of the system takes the value $\Delta A = 0.1A$, $\Delta B = 0.1B$, $\Delta A_d = 0.1A_d$. The element in the external disturbance $w(k)$ takes a Gaussian white noise with a mean of zero, $f(k) = 1.5 + \begin{bmatrix} 0.3\sin(6k) & 0 & 0.2\sin(2k) \end{bmatrix} x(k)$ is fault function. Time-varying delay $\tau(k)$ is a random integer between $[0, 5]$, $\sigma = \begin{bmatrix} 1 & 1 & 1 \end{bmatrix}$ is sliding model coefficient matrix, $x(0) = \begin{bmatrix} 1 & 1 & 1 \end{bmatrix}^T$ is the initial state of the whole system. This paper chooses the prediction horizon $P = 4$ and chooses control horizon $M = 2$, which takes account of both the fast and the stability of the system. Sampling time $k = 0.02$ and simulation time domain $k = 500$.

5.2. **Optimization algorithm comparison.**

Pseudo-code of the WOA algorithm

Initialize the whales population X_i $(i = 1, 2, \ldots, n)$

Calculate the fitness of each search agent

$\vec{X}^*$ = the best search agent

While ($t <$ maximum number of iterations)

  For each search agent

  Update $\vec{a}$, $\vec{A}$, $\vec{C}$, l, ρ

    For $i = 1$ to n do

      If ($\rho < 0.5$) then

If $\left(\left|\vec{A}<1\right|\right)$
$\vec{D}=\left|\vec{C}\vec{X}^{*}-\vec{X}_{i}\right|$
$\vec{X}_{i(j)}=\vec{X}^{*}(j)-\vec{A}\vec{D}$
Else if $\left(\left|\vec{A}\right|\geq 1\right)$
Select a random individual $\vec{X}_{rand}$
$\vec{D}=\left|\vec{C}\vec{X}_{rand}-\vec{X}_{i}\right|$
$\vec{X}_{i(j)}=\vec{X}_{rand}(j)-\vec{A}\vec{D}$
End if
Else if $(\rho\geq 0.5)$ then
$\vec{D}'=\left|\vec{X}^{*}-\vec{X}_{i}\right|$
$\vec{X}_{i(j)}=\vec{D}'e^{bl}\cos(2\pi l)+\vec{X}^{*}$
End if
End for
Evaluate the fitness for $\vec{X}_{i}$
End for
End while

Above, is the pseudo-code of the WOA. Now, this section selects four sets of benchmark functions to compare the particle swarm optimization algorithm with the whale optimization algorithm. The basic information of the four benchmark functions is shown in Table 1 (where, F_1, F_2 are unimodal functions, F_3, F_4 are multimodal functions).

TABLE 1. Information of benchmark functions

Function expression	Variable interval
$F_1=\sum_{i=1}^{N} i{x_i}^2$	$[-10,10]^{10}$
$F_2=\sum_{i=1}^{N} 10^{(6(i-1)/N-1)}{x_i}^2$	$[-100,100]^{10}$
$F_3=\sum_{i=1}^{N-1}\left(0.5+\frac{\sin^2\left(\sqrt{100x_i^2+x_{i+1}^2}\right)-0.5}{1+0.001\left(x_i^2-2x_ix_{i+1}+x_{i+1}^2\right)^2}\right)^2$	$[-100,100]^{10}$
$F_4=1-\cos\left(2\pi\sqrt{\sum_{i=1}^{N}x_i^2}+0.12\pi\sqrt{\sum_{i=1}^{N}x_i^2}\right)$	$[-100,100]^{10}$

The experiments were carried out independently for 30 times, and the average values, standard deviation, maximum, and minimum of the optimal target values of 30 experiments were used as the basis for performance evaluation. The number of search individuals and the maximum number of iterations for WOA and PSO are set to 10 and 50. WOA parameter setting: logarithmic spiral shape constant $b=1$. PSO parameter setting: attenuation coefficient $\varpi=1$, local learning factor, global learning factor $c_1=c_2=2.0$. The experimental results are shown in Table 2.

5.3. **Comparison of two sliding mode prediction algorithms.** For the quad-rotor helicopter system with time delay, uncertainty and fault, the control algorithm of this paper and the control algorithm of the paper [17] are used for experiments. The experimental results are shown in Figure 1 to Figure 4. It can be obtained from the experimental results that the control method designed in this paper is superior to the control algorithm proposed in [17] in terms of convergence speed, control precision and stability.

TABLE 2. Comparison on experimental results based on WOA and PSO

Function	Evaluation index	PSO	WOA
F_1	*mean*	1.00×10^{1}	8.79×10^{-46}
	std	5.48×10^{1}	4.79×10^{-45}
	max	3.00×10^{2}	2.62×10^{-44}
	min	9.60×10^{-3}	1.15×10^{-57}
F_2	*mean*	2.01×10^{7}	4.05×10^{-42}
	std	8.62×10^{7}	1.59×10^{-41}
	max	4.66×10^{8}	7.72×10^{-41}
	min	1.39×10^{5}	3.86×10^{-52}
F_3	*mean*	1.18×10^{0}	0.8361×10^{0}
	std	2.53×10^{-1}	0.4866×10^{0}
	max	1.75×10^{0}	1.5066×10^{0}
	min	7.11×10^{-1}	0.00×10^{0}
F_4	*mean*	4.47×10^{-7}	4.05×10^{-9}
	std	6.77×10^{-7}	1.69×10^{-8}
	max	3.40×10^{-6}	9.10×10^{-8}
	min	5.56×10^{-10}	1.88×10^{-15}

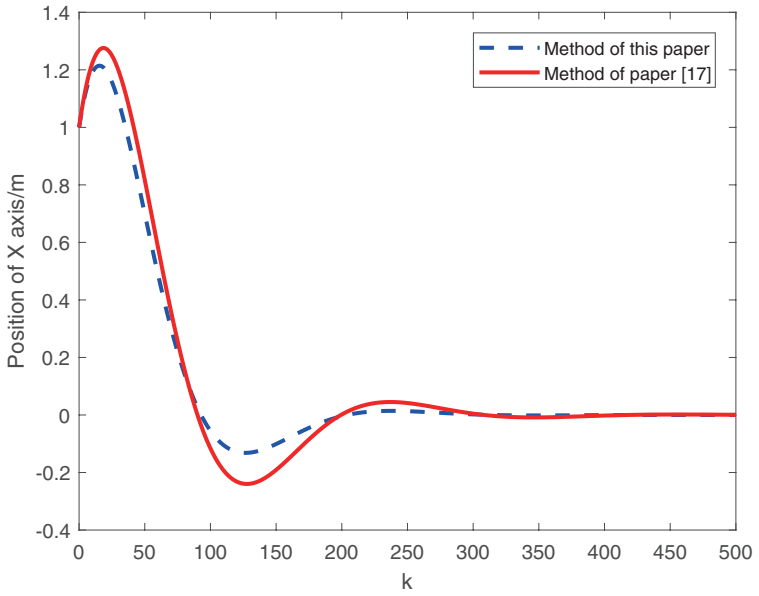

FIGURE 1. The position trajectories of X-axis

The position trajectory in Figure 1 indicates that the control method in this paper makes the quad-rotor helicopter more stable and smooth in the event of a fault.

Comparing the control rate trajectories in Figure 3 and Figure 4, we can clearly conclude that the convergence speed and accuracy are significantly improved due to the design of the whale optimization algorithm in the process of rolling optimization. And because the power function reference trajectory is designed, the method designed in this paper has excellent effect on the reduction of chattering.

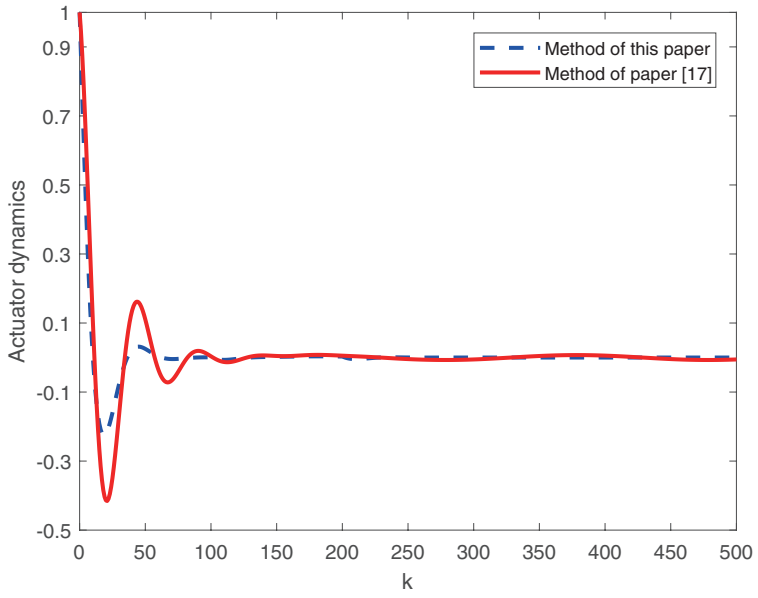

FIGURE 2. The actuator dynamics trajectories of X-axis

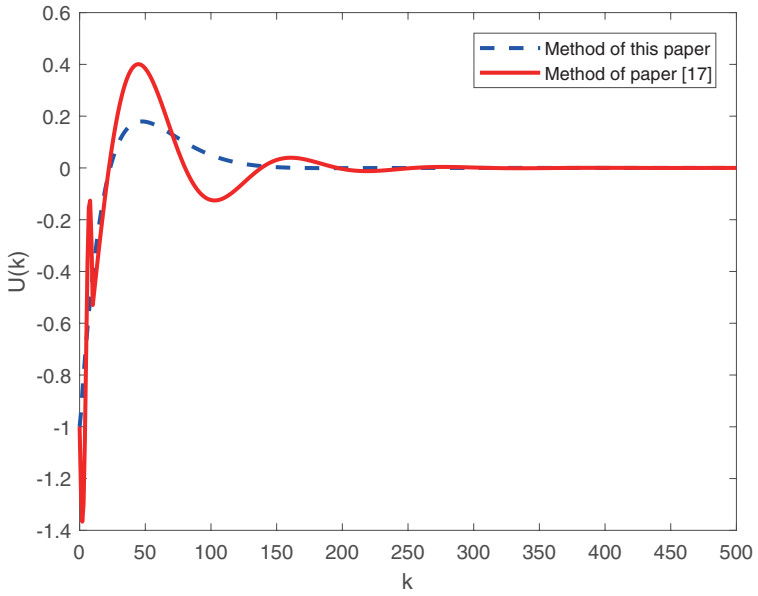

FIGURE 3. The trajectories of control law (1)

Therefore, by comprehensive comparison of the above simulation waveform, we can make the following summary and analysis. Firstly, compared with the paper [17], the method designed in this paper has obvious advantages in robustness and stability. The reason for this advantage is that a new global sliding mode switching function is designed in this paper, which eliminates the sliding mode approach process and avoids the instability of the approach process. Secondly, there are obvious differences between the two algorithms in convergence speed. In the process of rolling optimization, this paper designed a new optimization method to replace the particle swarm optimization algorithm. The whale optimization algorithm has the advantages of simple design, fast convergence

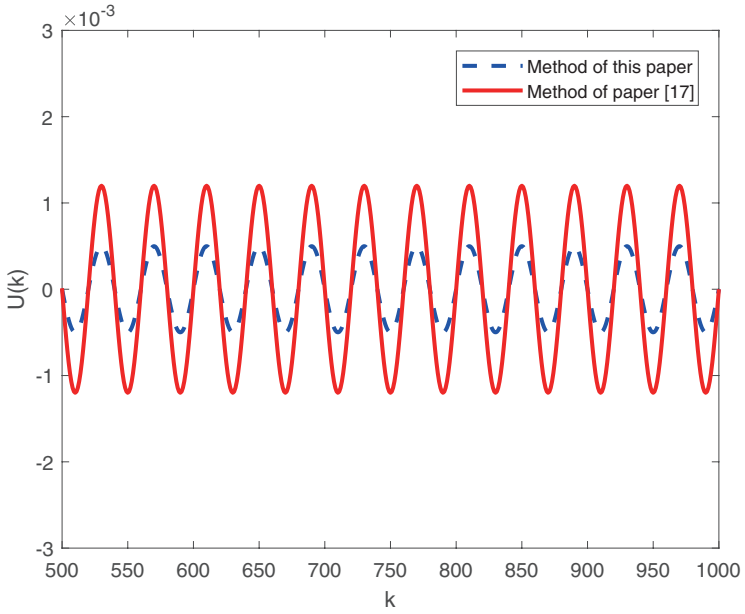

FIGURE 4. The trajectories of control law (2)

speed and high convergence accuracy, which have been reflected in the above simulation waveform. Finally, the chattering of the control law obtained in this paper is significantly reduced. Chattering was cut by nearly 50%. This is because a new type of reference trajectory is designed, which is used to compensate for the negative effects of faults and uncertainties. At the same time, the power function part of the reference track also has a good chattering suppression effect.

6. **Conclusion.** Combining the advantages of two control algorithms, sliding mode control and predictive control, this paper designs a sliding mode predictive control method based on whale optimization algorithm. And it solves the problem of fault-tolerant control of discrete uncertain systems with time-varying delays and disturbances, and achieves good control effects. The simulation results show that the proposed method has faster convergence speed and better robustness than paper [17]. In view of the instability phenomenon of the sliding mode approaching process and the sliding mode chattering problem, the general control method has not been deeply considered. In this paper, the problem is analyzed and processed, and a solution with better processing effect is designed. Of course, this article does not take into account the input time lag, and we will discuss this issue in future research.

Acknowledgment. The authors thank the anonymous reviewers for their useful comments that improved the quality of the paper. This work is supported by National Key Laboratory of Science and Technology on Helicopter Transmission (Nanjing University of Aeronautics and Astronautics) (No. HTL-O-19G11) and State Key Laboratory of Reliability and Intelligence of Electrical Equipment (No. EERIKF2018012), Hebei University of Technology, and the Fundamental Research Funds for the Central Universities (Nos. NS2017018, NJ20160025).

REFERENCES

[1] D. Ye and G. H. Yang, Adaptive fault-tolerant control for a class of nonlinear systems with time delay, *International Journal of Systems Science*, vol.39, no.1, pp.43-56, 2008.

[2] Z. Gao, P. Yang and M. Qian, Iterative learning observer-based fault tolerant control approach for satellite attitude system with mixed actuator faults, *ICIC Express Letters*, vol.13, no.7, pp.635-643, 2019.
[3] C. Li, S. Tong and Y. Wang, Fuzzy adaptive fault tolerant sliding mode control for SISO nonlinear systems, *International Journal of Innovative Computing, Information and Control*, vol.4, no.12, pp.3375-3383, 2008.
[4] M. Van, S. S. Ge and H. Ren, Robust fault-tolerant control for a class of second-order nonlinear systems using an adaptive third-order sliding mode control, *IEEE Trans. Systems, Man, and Cybernetics Systems*, vol.47, no.2, pp.221-228, 2017.
[5] S. Wang and J. Cui, Sensor-fault detection, diagnosis and estimation for centrifugal chiller systems using principal-component analysis method, *Applied Energy*, vol.82, no.3, pp.197-213, 2005.
[6] G. Hoblos, M. Staroswiecki and A. Aitouche, Optimal design of fault tolerant sensor networks, *IEEE International Conference on Control Applications*, 2018.
[7] J. Wang and Y. Wang, Dynamic programming technique in multi UAVs formation anomaly detection, *International Journal of Innovative Computing, Information and Control*, vol.14, no.6, pp.1977-1991, 2018.
[8] P. Yang, P. Xu and J. Liu, Optimal fault-tolerant control for UAV systems with time delay and uncertainties over wireless network, *Peer-to-Peer Networking and Applications*, vol.10, no.3, pp.1-9, 2016.
[9] W. D. Zhou, L. Zheng and C. Y. Liao, Sliding-mode predictive control for a class of uncertain discrete time-varying system, *The 3rd International Conference on Instrumentation*, 2014.
[10] H. B. Mansour, K. Dehri and A. S. Nouri, Discrete predictive sliding mode control for multivariable systems, *IEEE International Conference on Sciences and Techniques of Automatic Control and Computer Engineering*, 2015.
[11] L. Liu, Z. Wang and H. Zhang, Adaptive fault-tolerant tracking control for MIMO discrete-time systems via reinforcement learning algorithm with less learning parameters, *IEEE Trans. Automation Science and Engineering*, vol.14, no.1, pp.299-313, 2017.
[12] R. R. Nair and L. Behera, Robust adaptive gain higher order sliding mode observer based control-constrained nonlinear model predictive control for spacecraft formation flying, *IEEE/CAA Journal of Automatica Sinica*, vol.5, no.1, pp.370-384, 2018.
[13] B. M. Houda, A. Nizar and N. A. Said, Predictive sliding mode control for perturbed discrete delay time systems: Robustness analysis, *International Conference on Electrical Engineering and Software Applications*, 2013.
[14] Y. Peng, W. Wei and J. Wang, Model predictive control of time-delayed restraint system based on neurodynamical optimization, *Chinese Journal of Scientific Instrument*, vol.34, no.5, pp.961-966, 2013.
[15] S. Xie, C. Chen, L. Zhou, Z. Miao, X. Zhai and Z. Zhang, Sliding mode optimum predictive control for aero-engine based on time-delay compensator, *Control Engineering of China*, vol.19, no.5, pp.1671-7848, 2012.
[16] H. Gao and Y. Cai, Sliding mode predictive control for hypersonic vehicle, *Journal of Xi'an Jiaotong University*, vol.48, no.1, pp.67-72, 2014.
[17] P. Yang, R. Guo and X. Pan, Study on the sliding mode fault tolerant predictive control based on multi agent particle swarm optimization, *International Journal of Control, Automation and Systems*, vol.15, no.5, pp.2034-2042, 2017.
[18] Y. Zhu, S. Zhu, M. Xiao et al., The global sliding mode control for seat suspension system based on unmatched disturbance observer, *Journal of Vibration Engineering*, vol.27, no.5, pp.654-660, 2014.
[19] S. Mirjalili and A. Lewis, The whale optimization algorithm, *Advances in Engineering Software*, vol.95, pp.51-67, 2016.
[20] A. Chamseddine, T. Li, Y. Zhang, C. A. Rabbath and D. Theilliol, Flatness-based trajectory planning for a quadrotor unmanned aerial wehicle test-bed considering actuator and system constraints, *American Control Conference*, Montreal, Canada, pp.920-925, 2012.
[21] Q. P. Ha, H. Trinh, H. T. Nguyen et al., Dynamic output feedback sliding-mode control using pole placement and linear functional observers, *IEEE Trans. Industrial Electronics*, vol.50, no.5, pp.1030-1037, 2003.